7 December 2001

Chemical Physics Letters 349 (2001) 351–357

CHEMICAL PHYSICS LETTERS

www.elsevier.com/locate/cplett

On energy transfer processes at cluster–oxide interfaces: silver on titania

N. Nilius *, N. Ernst, H.-J. Freund

Fritz-Haber-Institut der Max-Planck-Gesellschaft Faradayweg 4-6, D 14195 Berlin, Germany

Received 28 August 2001

Abstract

Using a scanning tunneling microscope, electron-stimulated photon emission spectra have been measured for individual Ag clusters on differently pretreated TiO_2(1 1 0) substrates. For clusters on weakly reduced TiO_2, we observe radiating decays of Mie-plasmons shifting to higher energies as cluster sizes decrease. On strongly reduced TiO_2, plasmons are dissipated via energy transfer to electron–hole pair excitations in the oxide and emission spectra reveal radiating decays of TiO_2 excitons. © 2001 Elsevier Science B.V. All rights reserved.

Photo-catalytic processes on surfaces have attracted a growing interest in the research field of heterogeneous catalysis in recent years [1]. In contrast to thermal catalysis, photo-catalytic reactions can be activated at ambient temperature by creating electron–hole pairs in the photo-sensitive material after light irradiation. The hot electrons are transferred from the conduction band of the photo-catalyst into adsorbed molecular species, thus stimulating redox-reactions at the surface. Because of its band gap of 3 eV, TiO_2 turned out to be an ideal photo-catalytic material, easily to be activated by absorption of UV-light. Consequently, TiO_2-based photo-catalysts can be found in various technological applications, for instance in purification reactions of water and air [1,2], in the syntheses of organic molecules [3] and in the photo-catalytic dissociation of water [4]. After deposition of metal nanoparticles, for instance of Pt clusters, an increase of catalytic activity has been observed on TiO_2 surfaces [3,5]. The effect was attributed to two different mechanisms: (i) A local band-bending, induced by the metal nanoparticle, attracts hot electrons created after light absorption and increases the lifetime of the excited state. (ii) The metal cluster enhances the formation rate of electron–hole pairs in TiO_2 due to an additional energy transfer from the excited nanoparticle. Whereas the former process has been widely investigated for different cluster materials using XPS and UPS [6,7], little is known about the energy exchange between cluster and oxide. The problem is additionally complicated by the marked dependence of the coupling efficiency on cluster

* Corresponding author. Present address: University of California, Irvine 4129 Frederick Reines Hall Irvine, CA 92697, USA. Fax: +1-949-824-2174.

E-mail address: nilius@fhi-berlin.mpg.de (N. Nilius).

0009-2614/01/$ - see front matter
PII: S0009-2614(01)01232-5

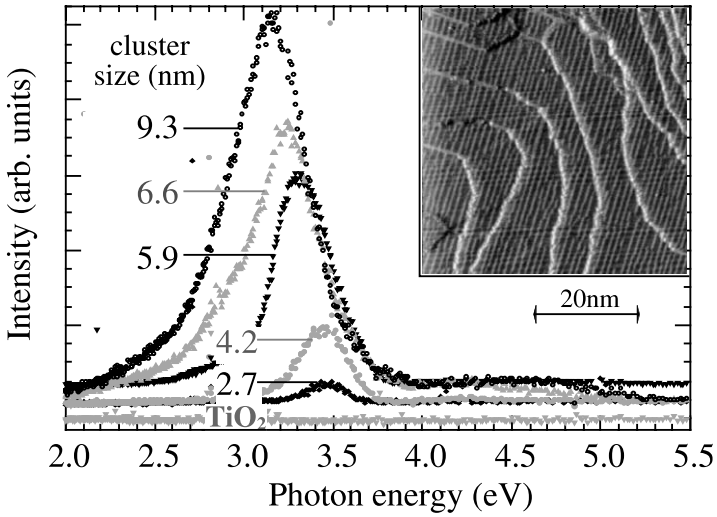

Fig. 1. Photon emission spectra of differently sized Ag clusters on weakly reduced $TiO_2(1\,1\,0)$, obtained for −10 V tip bias and 2 nA tunnel current. The inset shows an STM image of clean $TiO_2(1\,1\,0)$.

size, which demands for a local experimental technique to avoid inhomogeneous broadening effects caused by the cluster size distribution on the surface.

To address this question, we have excited individual Ag clusters deposited on a $TiO_2(1\,1\,0)$ surface in a controlled manner, using the electron current from an STM tip. The subsequent decay of the cluster excitation via substrate induced channels could directly be followed in the photon emission, stimulated by radiating recombinations of electron–hole pairs induced in TiO_2. The cluster–oxide coupling was measured as a function of cluster size and reduction-state of TiO_2. Ag particles have been chosen because of their well characterized, collective electronic excitation above 3 eV (Mie-plasmon), representing a defined starting point for energy transfer processes into the oxide.

In the experiment, light emission from individual Ag clusters was stimulated by the electron current from an STM tip. Emitted photons were collected by a parabolic mirror surrounding the STM and detected outside the UHV-chamber with a CCD camera attached to an UV/VIS spectrograph [8]. To minimize the electromagnetic coupling between tip and cluster a relatively large tip voltage (−10 V) and low electron currents (2 nA) have been employed to excite the cluster. Under these conditions, the tip–sample separation ranged between 1.5 and 2 nm and the electron beam was exclusively injected into a single cluster. For spectroscopic measurements, Ag particles were selected from topographic images. After completing a spectroscopic run, an STM image was taken for comparison to exclude morphological changes of the cluster during the experiment. To correct measured cluster sizes for the influence of tip convolution, an effective tip radius was derived from the apparent broadening of substrate step edges. The $(1\,1\,0)$-oriented TiO_2 single crystals have been prepared in two different ways. (i) Annealing to 1000 K in UHV for 5 min produces a weakly reduced crystal, characterized by a light blue color. (ii) Extension of the annealing time to 30 min, accompanied by a continued oxygen release from the bulk, leads to a strongly reduced, dark blue crystal [9]. After heat treatments, a clean $TiO_2(1\,1\,0)$ surface was prepared by cycles of Ar-sputtering and annealing to 800 K. For both preparation procedures, the long range order of the surface has been proven by a sharp (2×1)-LEED pattern and STM images, characterized by large terraces covered with parallel white lines (inset Fig. 1). The observed topographic structure is compatible with an added row model of Ti_2O_3-stripes running in [0 0 1]-direction along the sur-

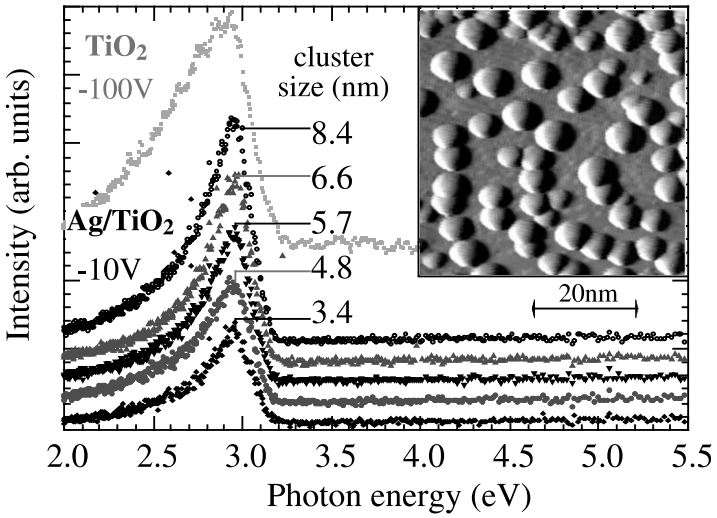

Fig. 2. Photon emission spectra of differently sized Ag clusters on strongly reduced $TiO_2(1\,1\,0)$ ($U_{tip} = -10$ V, $I = 2$ nA) and of clean TiO_2 ($U_{tip} = -100$ V, $I = 10$ nA). The inset shows an STM image of $Ag/TiO_2(1\,1\,0)$.

face [10]. Ag particles were prepared at room temperature by atom deposition from the gas phase. Nucleation to three-dimensional aggregates occurred preferentially at substrate step edges, resulting in a mean cluster density of 4×10^{-11} cm^{-2} (inset Fig. 2) [11,12].

On clean TiO_2 no light emission is detected at moderate tip voltages (Fig. 1, data on bottom), whereas the injection of 100 eV electrons from the tip into the oxide leads to a characteristic photon emission spectrum (Fig. 2, data on top). The emission behavior is determined by a gradual increase of the light intensity starting at 2 eV and a sudden drop above 2.9 eV. The intensity loss on the high-energy side of the spectrum corresponds to the TiO_2 bandgap of 3.03 eV. Based on photoluminescence measurements, this emission was interpreted as an interplay between radiating Mott–Wannier excitons at 2.9 eV and light emission from color centers at 2.3 eV localized at the oxide surface [13,14]. In contrast to the clean oxide, photon emission from silver particles can already be stimulated by electron injection at low tip bias (−10 V). Fig. 1 shows emission spectra for differently sized clusters, deposited on weakly reduced TiO_2. The spectra are dominated by a single, nearly symmetric emission peak around 3.2 eV, shifting to higher energies and losing intensity as cluster sizes decrease. Line widths in Fig. 1 are additionally broadened due to the finite resolution of the spectrograph. Homogeneous line widths of approximately 200 meV are obtained with higher spectral resolution. The emission behavior changes completely for silver particles deposited on strongly reduced TiO_2 (Fig. 2). In this case, a decreasing cluster size has no effect on the energy position of the emission line, remaining constant at 2.9 eV. A characteristic intensity increase with growing cluster diameter is observed for silver on strongly as well as on weakly reduced TiO_2. The different size dependences of the Ag emission peak are clearly discernible in Fig. 3.

The observed photon emission from Ag clusters on weakly reduced TiO_2 shows characteristic properties of radiating decays of Mie-plasmons, to be viewed as collective oscillations of the electron gas in small particles [15]. The peak at 3.1–3.5 eV can only be stimulated by electron injection into the cluster at negative tip polarity and is detected even at large tip–sample separations. Both observations are not compatible with an emission process based on the radiating decay of tip induced plasmons in the tunnel cavity, whereby the emission is determined by electromagnetic interactions

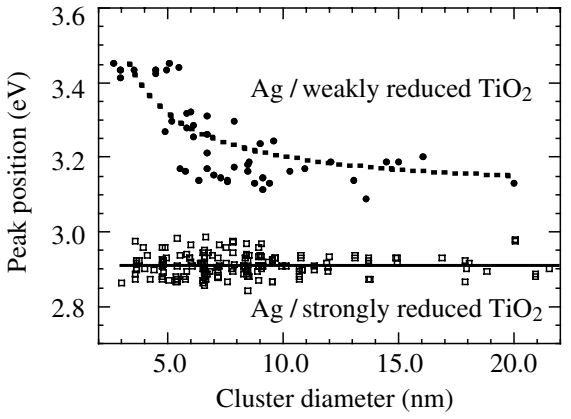

Fig. 3. Energy positions of photon emission peaks from Ag clusters on weakly and strongly reduced TiO_2 as a function of cluster diameter.

between tip and sample [16,17]. On the other hand, similar resonance positions have been identified for Mie-plasmons of Ag cluster ensembles in different embeddings using optical spectroscopies [18–20]. At present experimental conditions, only the plasmon dipole oriented perpendicular to the substrate (1, 0 mode) can be excited by electrons injected from the STM tip. The energy $\hbar\omega$ of the observed emission peak from Ag/TiO_2 shows a blueshift for decreasing cluster diameter d, which can be fitted with the functional relation: $\hbar\omega(d) = 3.1\ \text{eV} + 0.76\ \text{eV nm}/d\ (\text{nm})$ (Fig. 3). Comparable blueshifts have been found for the 1, 0 mode of Mie-plasmons in Ag clusters deposited on $Al_2O_3/NiAl$ (110) [21] or embedded in Ar, Ne and Kr matrices [22]. The blueshift of the Mie-energy with decreasing cluster size was interpreted as a consequence of the reduced screening of the plasmon by silver d-electrons at the cluster surface [23]. The growing weight of this surface effect with respect to bulk properties is responsible for the d^{-1} dependence of the plasmon frequency in small particles. The additive constant of 3.1 eV in the size dependence for Ag/TiO_2 corresponds to the energy position of the 1, 0 Mie-mode in larger particles. The value can be estimated from the resonance condition for the polarizability of metal spheroids in dielectric media [24]

$$\varepsilon_{Ag}(\omega) = -\varepsilon_m(1 - L_\perp)/L_\perp. \quad (1)$$

Here, ε_{Ag} is the dielectric function of silver [25] and ε_m describes the cluster environment consisting of 30% TiO_2 ($\varepsilon_{TiO_2} = 7.5$) and 70% vacuum. Using a depolarization factor $L_\perp$ of 0.4, accounting for the oblate cluster shape derived from STM images, a plasmon energy of 3.0 eV is calculated for large particles in agreement with experiment.

Asymmetric emission lines from Ag particles, measured on strongly reduced TiO_2, cannot be explained by the well-known properties of Mie-plasmons [15]. From Eq. 1, the smaller resonance frequency of 2.9 eV is obtained only for a higher ε_m, equivalent to more than 50% Ag/TiO_2 interface. For preparation conditions at room temperature, a penetration of the cluster into the substrate or very flat particle shapes can be excluded. Also, the size dependence of the peak position, predicted for a radiating decay of Mie-plasmons, is not observed for particles on strongly reduced TiO_2. However, the similar behavior of the emitted intensity as a function of cluster diameter on both substrates indicates an influence of collective excitations in Ag clusters on the emission process for strongly reduced TiO_2 as well. On both substrates, the photon yield increases proportional to cluster volume (d^3), reflecting the dependence of the plasmon oscillator strength on the number of electrons involved in the collective excitation [15]. Based on these arguments, the following mechanism is proposed for the emission process from silver on strongly reduced TiO_2. The Mie-plasmon, excited in a single Ag cluster by electrons from the tip, is dissipated in the TiO_2 crystal on a time scale, too short to allow for a detectable photon emission rate. The released plasmon energy of approximately 3.2 eV is transferred to electron–hole pair excitations in the oxide bandgap. The radiating recombination of coupled electron–hole pairs in TiO_2 gives rise to the observed emission peak at fixed photon energy for all cluster sizes. This interpretation is strongly supported by the emission properties of the clean oxide upon irradiation with 100 eV electrons, which agrees with the emission from Ag particles on strongly reduced TiO_2 stimulated with 10 eV electrons (Fig. 2). For low electron energies, the photon yield from electron–hole pair recombinations is considerably higher for the plasmon mediated channel (Ag/reduced TiO_2)

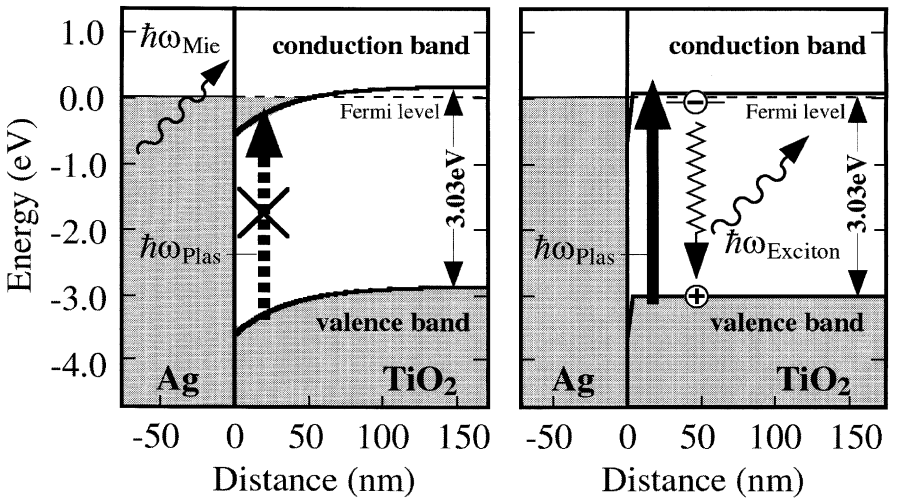

Fig. 4. Energy diagram of the Ag/TiO_2 interface. To estimate screening lengths, electron densities in the oxide conduction band of 1016 cm^{-3} for weakly (left) and 1020 cm^{-3} for strongly (right) reduced TiO_2 have been assumed.

than for a direct electronic stimulation of the clean oxide. In the absence of an Ag particle in the STM cavity, tunneling events create (i) holes in the valence band of TiO_2 at positive tip bias or (ii) hot electrons in the conduction band at negative polarity. In both cases, the density of either (i) free electrons in the conduction or (ii) holes in the valence band is too small to produce detectable cross-sections of radiating recombinations. The probability for photon emission processes is additionally reduced due to the indirect bandgap of TiO_2. Only after injection of high-energy electrons (100 eV), a sufficient number of secondary electrons and holes is excited in TiO_2, enabling to stimulate measurable photon yields from the clean oxide. In contrast, the decay of Mie-plasmons in supported Ag particles directly creates coupled electron–hole pairs in the oxide. These excitons are confined in space by Coulomb attraction and have an enhanced probability for a radiating recombination. Higher photon yields can therefore be expected for plasmon mediated processes.

Finally, the role of the reduction-state of the TiO_2 substrate has to be discussed. While radiating decays of Mie-plasmons are observed for Ag clusters on almost stoichiometric TiO_2, the intrinsic oxide emission dominates the spectra of Ag particles on strongly reduced crystals. An explanation for this behavior is deduced from the electronic properties of the metal–oxide interface, characterized by bending of the oxide bands. In the Schottky limit [26], the effect can be estimated from the different work functions of silver ($\phi = 4.7$ eV) [27] [1] and $TiO_2(1\,1\,0)$ ($\phi = 5.3$ eV) [28,29]. In the model, the lower metal work function leads to a local downward bending of the oxide bands of approximately 0.6 eV and to a quantum well formation at the Ag/TiO_2 interface. A similar behavior has been derived from UPS and XPS studies after the preparation of larger Au and Pt particles on TiO_2 [6]. As the quantum well is filled with electrons up to the Fermi level of the system, an additional amount of energy is required to excite an electron from the TiO_2 valence band to unoccupied states in the quantum well (Fig. 4). At the metal–oxide interface, the formation energy of electron–hole pairs of approximately 3.6 eV (band gap plus quantum well depth) is therefore higher than the maximum Mie-plasmon energy of 3.5 eV. At a temperature T, the band bending is screened

[1] Hereby, we assume the formation of Ag(1 1 1) facets at the interface, in correspondence to other cluster–TiO_2(1 1 0) systems [34].

by electrons in the conduction band at a scale of the Debye length L_d with

$$L_d^2 = (kT\varepsilon_0\varepsilon_{TiO_2})/(2e^2n) \quad (2)$$

(cf. [30,31]). Hereby, k is the Boltzmann constant and ε_0 the permittivity of vacuum. The electron density n in TiO_2 can be estimated from crystal color and preparation conditions [32,33]. For our qualitative model, a carrier density in the order of 10^{16} cm^{-3} is assumed for the weakly reduced oxide. According to Eq. 2, the quantum well extends approximately 25 nm into the TiO_2 below an Ag particle and efficiently suppresses the coupling between Mie-plasmons and oxide excitons in this volume (Fig. 4, left). Consequently, Ag-plasmons are not dissipated on weakly reduced oxide samples and the characteristic photon emission from single Ag particles can be observed. We note that the model remains valid also for a TiO_2 electron density of 10^{17} cm^{-3}, when the screening length is reduced to approximately 8 nm. Strongly reduced, deep blue crystals are characterized by an approximate carrier density of 10^{19}–10^{20} cm^{-3} [33], leading to an efficient screening of the band bending on a length scale of 0.5 nm. The surface quantum well almost disappears and the initial TiO_2 bandgap energy of 3.03 eV is sufficient to excite electron–hole pairs at the metal–oxide interface. At these conditions, the formation of excitons in the oxide becomes the dominant decay channel for Mie-plasmons in Ag clusters of all sizes (Fig. 4, right). Photon emission spectra from particles on strongly reduced TiO_2 are consequently determined by the 2.9 eV emission line from radiating decays of TiO_2 excitons and the Mie-plasmon peak at 3.1–3.5 eV is no longer observable.

In conclusion, we have examined the electron-stimulated photon emission from individual Ag clusters, supported on differently prepared $TiO_2(1\,1\,0)$ surfaces. Due to the high-lateral resolution of the STM-based method, a different emission behavior of single particles as a function of size could be established for weakly and strongly reduced oxide substrates. On weakly reduced TiO_2, the emission from Ag particles shows characteristics of radiating Mie-plasmons. In the limit of large clusters, a plasmon energy of 3.1 eV is determined in agreement with theoretical estimations. The resonance frequency shifts to higher values for decreasing cluster size. However, emission peaks from Ag clusters appear at constant photon energy of 2.9 eV for particles on strongly reduced TiO_2 crystals. Shape and position of the peaks agree with the intrinsic emission behavior of clean TiO_2, irradiated with 100 eV electrons. Based on these observations, an emission process is conceived, consisting of Mie-plasmon excitations in an Ag particle, energy transfer to electron–hole pairs in TiO_2 and radiating decays of these excitons in the bandgap. Consequently, the efficiency of the cluster–oxide coupling strongly depends on the band bending in TiO_2 after silver deposition, which in turn varies with the reduction-state of the oxide.

Acknowledgements

For financial support we are grateful to the Deutsche Forschungsgemeinschaft, the Fond der Chemischen Industrie and the NEDO Research Grant on Photon and Electron Controlled Surface Processes.

References

[1] G. Ertl, H. Knözinger, J. Weitkamp, in: Handbook of Heterogenous Catalysis, vol. 4, Wiley-Vch, Weinheim, 1997, p. 2111.
[2] D.E. Ollis, H. Al-Ekabi (Eds.), Photocatalytic Purification and Treatment of Water and Air, Elsevier, Amsterdam, 1993.
[3] P. Pichat, M.A. Fox, in: M.A. Fox, M. Channon (Eds.), Photoinduced Electron Transfer, Elsevier, Amsterdam, 1988.
[4] D. Brinkley, M. Dietrich, T. Engel, Surf. Sci. 395 (1998) 292.
[5] J.P. Bucher, J. Vanderklink, M. Graetzel, J. Phys. Chem. 94 (1990) 1209.
[6] L. Zhang, R. Persaud, T.E. Madey, Phys. Rev. B 56 (1997) 10549.
[7] C.T. Campbell, Surf. Sci. Rep. 27 (1997) 1.
[8] N. Nilius, A. Cörper, G. Bozdech, N. Ernst, H.-J. Freund, Prog. Surf. Sci. 67 (2001) 99.
[9] M. Li, W. Hebenstreit, L. Gross, U. Diebold, M.A. Henderson, D.R. Jennison, P.A. Schultz, M.P. Sears, Surf. Sci. 437 (1999) 173.

[10] H. Onishi, Y. Iwasawa, Phys. Rev. Lett. 76 (1996) 791.
[11] K. Luo, T.P. Clair, X. Lai, D.W. Goodman, J. Phys. Chem. B 104 (2000) 3050.
[12] P.W. Murray, J. Shen, N.G. Condon, S.J. Pang, G. Thornton, Surf. Sci. 380 (1997) L455;
Z. Chang, S. Haq, G. Thornton, Surf. Sci 467 (2000) L841.
[13] A. Amtout, R. Leonelli, Sol. Stat. Commun. 84 (1992) 349.
[14] L. Forss, M. Schubnell, Appl. Phys. B 56 (1993) 363.
[15] U. Kreibig, W. Vollmer, in: Optical Properties of Metal Clusters, Springer Series Materials Science, vol. 25, Springer, Berlin, 1995.
[16] P. Johansson, R. Monreal, P. Apell, Phys. Rev. B 42 (1990) 9210.
[17] R. Berndt, J.K. Gimzewski, P. Johansson, Phys. Rev. Lett. 67 (1991) 3796.
[18] U. Kreibig, L. Genzel, Surf. Sci. 156 (1985) 678.
[19] D. Martin, J. Jupille, Y. Borensztein, Surf. Sci. 402 (1998) 433.
[20] T. Wenzel, J. Bosbach, F. Stietz, F. Träger, Surf. Sci. 432 (1999) 257.
[21] N. Nilius, N. Ernst, H.-J. Freund, Phys. Rev. Lett. 84 (2000) 3994.
[22] K.-P. Charlé, L. König, S. Nepijko, I. Rabin, W. Schulze, Cryst. Res. Technol. 33 (1998) 1085.
[23] A. Liebsch, Phys. Rev. B 48 (1993) 11317.
[24] R. Gans, Ann. Phys. 37 (1912) 881.
[25] E.D. Palik (Ed.), Handbook of Optical Constants of Solids, Academic press, Orlando, 1985.
[26] W. Schottky, Z. Phys. 113 (1939) 367.
[27] J. Hölzl, F.K. Schulte, H. Wagner, in: Solid Surface Physics, Springer Tracts in Modern Physics, vol. 85, Springer, Berlin, 1979.
[28] V.E. Henrich, P.A. Cox, The Surface Science of Metal Oxides, Cambridge University Press, Cambridge, 1994.
[29] H. Onishi, T. Aruga, C. Egawa, Y. Iwasawa, Surf. Sci. 233 (1990) 261.
[30] W. Mönch, in: G. Ertl (Ed.), Semiconductor Surfaces and Interfaces, Springer Series in Surface Science, vol. 26, Springer, Berlin, 1993.
[31] C. Noguera, Physics and Chemistry at Oxide Surfaces, Cambridge University Press, Cambridge, 1995.
[32] M. Li, W. Hebenstreit, U. Diebold, A.M. Tyryshkin, M.K. Bowman, G. Dunham, M.A. Henderson, J. Phys. Chem. B 104 (2000) 4944.
[33] E. Iguchi, K. Yagima, T. Asahima, T. Kanamori, J. Phys. Chem. Sol. 35 (1974) 597.
[34] X. Lai, T.P. St Clair, M. Valden, D.W. Goodman, Prog. Surf. Sci. 59 (1998) 25.